

Magnetoresistance in high oxidation state iron oxides

P. D. Battle,^{*a†} M. A. Green,^a J. Lago,^a A. Mihut,^b M. J. Rosseinsky,^{*a†} L. E. Spring,^{a,b} J. Singleton^{*b} and J. F. Vente^a

^aInorganic Chemistry Laboratory, Department of Chemistry, University of Oxford, South Parks Road, Oxford, UK OX1 3QR

^bClarendon Laboratory, Department of Physics, University of Oxford, Parks Road, Oxford, UK OX1 3PU

Magnetoresistance is observed in non-ferromagnetic oxides containing Fe^{IV} which have magnetic behaviour characteristic of small magnetic clusters.

Much attention has recently been focused on the observation of colossal magnetoresistance (CMR, *i.e.* almost 100% suppression of the zero-field resistance upon application of a magnetic field) near the coincident Curie and metal–insulator transition temperatures of ferromagnetic manganese oxides.¹ Investigation of oxides of metals other than manganese has shown CMR { $\Delta\rho/\rho = [\rho(0) - \rho(B)]/\rho(0) < 72\%$ in 10 T} in ferromagnetic La_{1-x}Sr_xCoO₃² with a similar mechanism to that of the manganites being invoked, and $\Delta\rho/\rho = 4\%$ in a 7 T field at 150 K in the metallic ferromagnet SrRuO₃.³ $\Delta\rho/\rho = 20\%$ at 6 T in Cr-based chalcogenide spinels has recently been reported.⁴ We have been engaged in a search for magnetoresistance in first-row transition metal oxides,^{5,6} and report here the first observation of significant magnetoresistance ($\Delta\rho/\rho \leq 19\%$ in 12 T at 4.2 K) in iron-based oxides with significant cooperative magnetic interactions but no long-range ferromagnetic order. The systems were chosen as dilute solid solutions between the itinerant helical antiferromagnet SrFeO₃, the ferromagnetic metal SrCoO₃ and the valence-unstable CaFeO₃, which undergoes disproportionation into Fe^{III} and Fe^V.⁷

Perovskite oxides of composition SrFe_{0.9}Co_{0.1}O₃ and Sr_{0.9}Ca_{0.1}FeO₃ were prepared by solid state reaction of the starting oxides plus strontium carbonate in air at 1100 °C followed by annealing under 800 bar O₂ at 400 °C for three days to maximise the metal oxidation states.† Rietveld refinement of powder neutron and X-ray (from both laboratory and high resolution synchrotron sources) diffraction data showed that both products were undistorted pure cubic perovskites, with an oxygen content corresponding to a mean cation oxidation state of +IV. This was confirmed by TGA reduction under hydrogen. Magnetic measurements over a range of fields and temperatures indicate the presence of strong and competing exchange interactions, consistent with the strong covalency produced by the high metal oxidation states. The Curie–Weiss law is obeyed above 260 K with moments of 7.9 (Ca) and 9(Co) μ_B , significantly enhanced over the high-spin Fe^{IV} spin-only value of 4.9 μ_B in both cases, in agreement with previous work on SrFeO_{3.00}⁸ and SrFe_{0.9}Co_{0.1}O₃.⁹ The Weiss constant was significantly more positive for the Co doped phase (210 K *cf.* 10 K).

History-dependent measurements on SrFe_{0.9}Co_{0.1}O₃ at 100 G show a maximum in both field-cooled (FC) and zero-field cooled (ZFC) magnetisations at 85 K (Fig. 1). $M(H)$ is linear at 300 K but becomes sigmoidal in shape (without hysteresis) below 170 K and shows no sign of saturation in a 50 kG measuring field (Fig. 1 inset). These observations are consistent with the existence of cooperative magnetic interactions without long-range magnetic order, resulting in the formation of small magnetic domains often characterised as cluster glass behaviour.¹⁰ Mössbauer spectroscopy has previously suggested that the distribution of Co at low (<0.2) doping levels in SrFe_{1-x}Co_xO₃ is inhomogeneous, with Co-rich regions being ferromagnetic in a non-ferromagnetic matrix.^{11,12}

The magnetic behaviour of Sr_{0.9}Ca_{0.1}FeO₃ differs. The magnetisation is smaller than that of the Co-doped sample and decreases after a sharp maximum at 120 K. Neutron powder diffraction measurements (Fig. 2 inset) show that this coincides with the onset of antiferromagnetic long-range order with the

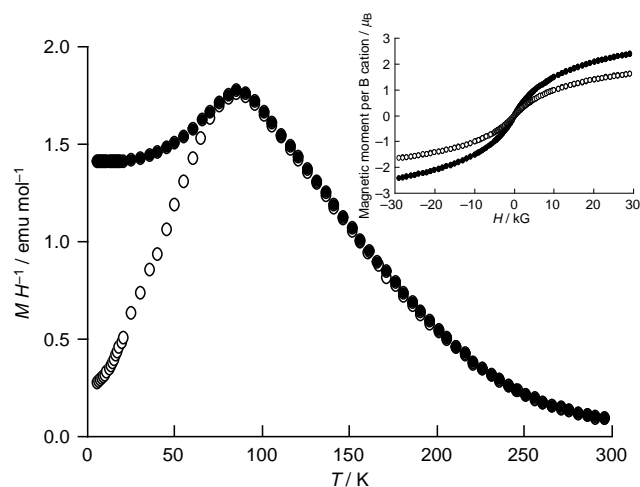


Fig. 1 Temperature dependence of M/H for SrFe_{0.9}Co_{0.1}O_{3.00} in a measuring field of 100 G. Field-cooled (FC) data are shown as filled circles, zero-field-cooled (ZFC) as empty circles. Inset: ZFC $M(H)$ isotherm of SrFe_{0.9}Co_{0.1}O_{3.00} at 45 K (filled circles) and 170 K. The sigmoidal shape indicates the existence of magnetic domains within the sample. $M(H)$ isotherms at different temperatures do not fall on a universal curve when plotted as a function of H/T , indicating the compound is not a classical superparamagnet.

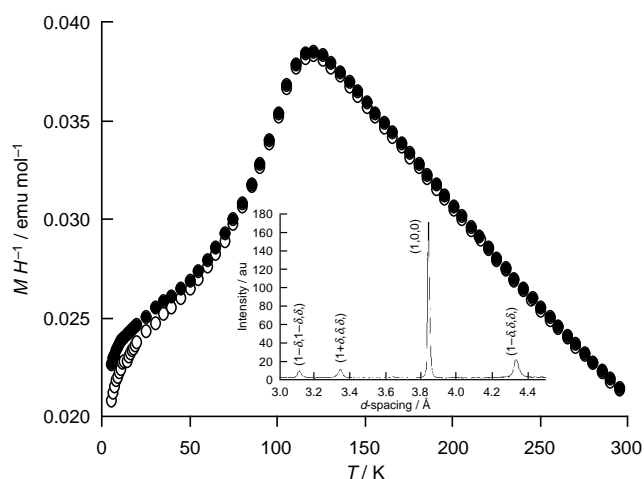


Fig. 2 Temperature dependence of M/H for Sr_{0.9}Ca_{0.1}FeO_{3.00} in a 100 G measuring field. Field-cooled (FC) data are shown as filled circles, zero-field-cooled (ZFC) as empty circles. Inset: incommensurate magnetic Bragg structure observed at 5 K (the nuclear (1 0 0) reflection is also shown.)

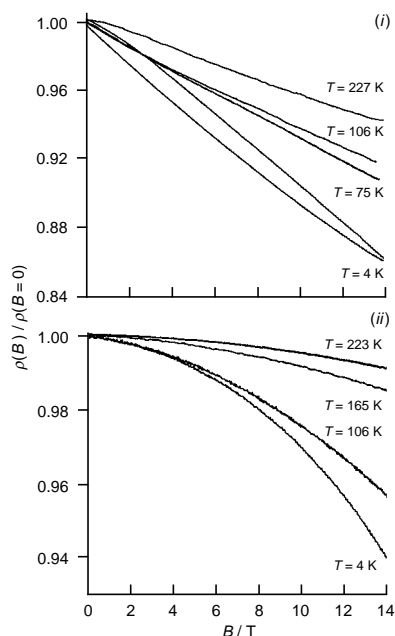


Fig. 3 Magnetoresistance isotherms of (i) $\text{SrFe}_{0.9}\text{Co}_{0.1}\text{O}_3$ and (ii) $\text{Sr}_{0.9}\text{Ca}_{0.1}\text{FeO}_3$

helical antiferromagnetic structure found for SrFeO_3 .¹³ There is, however, significant divergence between FC and ZFC data below 100 K (Fig. 2) suggesting the development of magnetic disorder at low temperatures. The adoption of a helical magnetic structure by SrFeO_3 in preference to one of the collinear structures common amongst perovskites,¹⁴ demonstrates that the competing interactions necessary to cause spin-glass behaviour are present in this system. Furthermore, the presence of a disordered Ca/Sr distribution will introduce an element of randomness into the superexchange interactions; this effect is likely to be relatively large, given the sharp contrast in the properties of SrFeO_3 and CaFeO_3 .

Despite the clear absence of a transition to a three-dimensionally ordered ferromagnetic state in the magnetisation measurements on either compound, significant magnetoresistance is observed for temperatures below 250 K (Fig. 3), with values of the conservative figure-of-merit $[\rho(B = 12 \text{ T}) - \rho(B = 0)]/\rho(B = 0)$ of 9% at 50 K for $\text{Sr}_{0.9}\text{Ca}_{0.1}\text{FeO}_3$ and 18% at 4 K for $\text{SrFe}_{0.9}\text{Co}_{0.1}\text{O}_3$ (11% at 100 K).

Powder neutron diffraction indicates a smooth structural evolution with temperature. The absence of a localised to itinerant electron transition signalled by ferromagnetism produced by double exchange and of structural features associated with strong Jahn–Teller electron–phonon coupling provides a clear distinction from the behaviour of mixed-valence manganates. The observation of both magnetic behaviour suggestive of ferromagnetically correlated inhomogeneities and magnetoresistance appears to be analogous to the behaviour of the heterogeneous, ferromagnetic Cu–Co and Ag–Co alloys which are some of the best ‘giant’ magnetoresistance (GMR) materials.¹⁵ In the alloys, the scattering of electrons at the grain boundaries between the ferromagnetic regions embedded in a conducting matrix is strongly reduced by the application of a magnetic field, which reduces the angle between the moments of the magnetic regions and suppresses spin-dependent scattering. The presence of ferromagnetic regions in the Co-doped system, seen by magnetisation isotherms to be present at temperatures where significant magnetoresistance is observed, may indicate that a similar mechanism operates in the present materials.

The magnetisation of both phases reported here suggests the presence of competing interactions and non-equilibrium behaviour due to cluster formation and blocking. The presence of

competing ferro- and antiferro-magnetic interactions is a common feature of the two ternary iron oxides presented here, and suggests that this recipe for significant, albeit not colossal, magnetoresistance in oxides deserves further exploration, a suitable starting point being the optimisation of the effect in the current system.

We thank the EPSRC for support including a studentship for L. E. S. and access to station 2.3 at Daresbury Laboratory, where C. C. Tang assisted us, and to the HRPD and IRIS instruments at ISIS. We are particularly indebted to R. M. Ibberson for his assistance at the ISIS facility. J. L. thanks the Basque Government (‘Gobierno Vasco-Eusko Jaurlarita’) for a studentship and M. J. R. thanks the Royal Society for a grant towards the cost of developing the high pressure oxygen apparatus.

Notes and References

† E-mail: matthew.rosseinsky@chem.ox.ac.uk; peter.battle@chem.ox.ac.uk

‡ The high oxygen pressure was generated by diaphragm compression of 200 bar oxygen using a Fluiftron compressor. The reaction mixture was contained in gold foil within an externally heated Rene 41 cold-seal vessel. X-Ray powder diffraction data were recorded using a Siemens D5000 diffractometer (Cu- $\text{K}\alpha_1$ radiation) in Bragg–Brentano geometry and also on station 2.3 of the Synchrotron Radiation Source, Daresbury Laboratory. Neutron powder diffraction data were recorded for $4 \leq T/\text{K} \leq 300$ on the high resolution diffractometer HRPD and on the long-wavelength IRIS instrument at the ISIS pulsed neutron source, Rutherford Appleton Laboratory. Rietveld refinement was carried out with the GSAS suite of programs. The refined compositions from the neutron data were $\text{SrFe}_{0.9}\text{Co}_{0.1}\text{O}_{3.00(1)}$ [$a = 3.84625(6) \text{ \AA}$] and $\text{Sr}_{0.9}\text{Ca}_{0.1}\text{FeO}_{2.99(1)}$ ($a = 3.84621(5) \text{ \AA}$), consistent with the observation that the cubic perovskite is only stable for oxygen content $2.97 \leq y \leq 3.00$ ¹⁶ and TG estimates of $y = 3.00 \pm 0.05$. Our synthetic method for SrFeO_3 gives $a = 3.85097(3) \text{ \AA}$. Magnetic measurements were made with a Quantum Design MPMS5 SQUID magnetometer. Magnetoresistance measurements were made using standard, low-frequency (31 Hz), four-wire ac techniques in fields of up to 14 T with the current (0.2 mA) perpendicular to the magnetic field.

- 1 A. P. Ramirez, *J. Phys.: Condens. Matter*, 1997, **9**, 8171.
- 2 G. Briceno, H. Chang, X. Sun, P. G. Schultz and X.-D. Xiang, *Science*, 1995, **270**, 273.
- 3 S. C. Gausepohl, M. Lee, K. Char, R. A. Rao and C. B. Eom, *Phys. Rev. B*, 1995, **52**, 3459.
- 4 A. P. Ramirez, R. J. Cava and J. Krajewski, *Nature*, 1997, **386**, 156.
- 5 P. D. Battle, S. J. Blundell, M. A. Green, W. Hayes, M. Honold, A. K. Klehe, N. S. Laskey, J. E. Millburn, L. Murphy, M. J. Rosseinsky, N. A. Samarin, J. Singleton, N. E. Sluchanko, S. P. Sullivan and J. F. Vente, *J. Phys. Condens. Matter*, 1996, **8**, L427.
- 6 P. D. Battle, M. A. Green, N. S. Laskey, J. E. Millburn, M. J. Rosseinsky, S. P. Sullivan and J. F. Vente, *Chem. Commun.*, 1996, 767.
- 7 T. Takeda, S. Naka, M. Takano, T. Shinjo, T. Takada and M. Shimada, *Mater. Res. Bull.*, 1978, **13**, 61.
- 8 J. B. MacChesney, R. C. Sherwood and J. F. Potter, *J. Chem. Phys.*, 1965, **43**, 1907.
- 9 S. Kawasaki, M. Takano and Y. Takeda, *J. Solid State Chem.*, 1996, **121**, 174.
- 10 K. Eftimova, R. Laiho, K. G. Lisunov and E. Lahderanta, *J. Magn. Mater.*, 1996, **154**, 193.
- 11 T. Takeda, T. Watanabe and S. Komura, *J. Phys. Soc. Jpn.*, 1987, **56**, 336.
- 12 T. Takeda, T. Watanabe, S. Komura and H. Fuji, *J. Phys. Soc. Jpn.*, 1987, **56**, 731.
- 13 T. Takeda, Y. Yamaguchi and H. Watanabe, *J. Phys. Soc. Jpn*, 1972, **33**, 967.
- 14 E. O. Wollan and W. C. Koehler, *Phys. Rev.*, 1955, **100**, 545.
- 15 A. E. Berkowitz, J. R. Mitchell, M. J. Carey, A. P. Young, D. Rao, A. Starr, S. Zhang, F. E. Spada, F. T. Parker, A. Hutten and G. Thomas, *J. Appl. Phys.*, 1993, **73**, 5320.
- 16 Y. Takeda, K. Kanno, T. Takada, O. Yamamoto, M. Takano, N. Nakayama and Y. Bando, *J. Solid State Chem.*, 1986, **63**, 237.

Received in Cambridge, UK, 12th February 1998; 8/01220B